Arabian Journal of Chemistry (2022) **15**, 104010

King Saud University

Arabian Journal of Chemistry

www.ksu.edu.sa
www.sciencedirect.com

ORIGINAL ARTICLE

Modification of silica nanoparticles with 1-hydroxy-2-acetonaphthone as a novel composite for the efficient removal of Ni(II), Cu(II), Zn(II), and Hg (II) ions from aqueous media

Asma S. Al-Wasidi [a], **Ahmed M. Naglah** [b,c], **Fawaz A. Saad** [d],
Ehab A. Abdelrahman [e,*]

[a] *Department of Chemistry, College of Science, Princess Nourah Bint Abdulrahman University, P.O. Box 84428, Riyadh 11671, Saudi Arabia*
[b] *Department of Pharmaceutical Chemistry, Drug Exploration & Development Chair (DEDC), College of Pharmacy, King Saud University, P.O. Box 2457, Riyadh 11451, Saudi Arabia*
[c] *Peptide Chemistry Department, National Research Centre, 12622-Dokki, Cairo, Egypt*
[d] *Department of Chemistry, Faculty of Applied Sciences, Umm Al-Qura University, Makkah 21955, Saudi Arabia*
[e] *Chemistry Department, Faculty of Science, Benha University, Benha 13518, Egypt*

Received 21 March 2022; accepted 24 May 2022
Available online 30 May 2022

KEYWORDS

Adsorption;
Heavy metals;
Nanocomposite;
1-hydroxy-2-acetonaphthone;
SiO_2 nanoparticles

Abstract In this paper, a novel composite based on the formation of Schiff base on silica nanoparticles was facilely synthesized. Firstly, silica nanoparticles, which contain silanol groups (Si-OH), were modified with (3-aminopropyl)trimethoxysilane. Then, the modified silica reacted with 1-hydroxy-2-acetonaphthone to form a novel Schiff base/silica composite. The synthesized composite was characterized using several tools such as XRD, FT-IR, FE-SEM, N_2 adsorption/desorption analyzer, and CHN analyzer. The considerable reduction at $2\theta = 21.9°$ in the intensity of the XRD peak of the composite is owing to the formation of the Schiff base. Also, the observed FT-IR bands in the composite at 3440 and 1604 cm^{-1} are owing to the stretching and bending vibrations of OH and/or C=N, respectively. The FE-SEM images confirmed that the silica includes irregular shapes whereas the composite possesses a flaky surface owing to the formation of the Schiff base. Elemental analysis of the composite demonstrated that the % C, % H, and % N are 15.26, 3.24, and 1.65 %, respectively. The BET surface area and total pore volume of the composite

---

* Corresponding author.
E-mail address: ehab.abdelrahman@fsc.bu.edu.eg (E.A. Abdelrahman).

Peer review under responsibility of King Saud University.

Production and hosting by Elsevier

https://doi.org/10.1016/j.arabjc.2022.104010

were reduced because the formed Schiff base blocks the pores of silica. The synthesized composite was employed for the efficient removal of Ni(II), Cu(II), Zn(II), and Hg(II) ions from aqueous media. The maximum uptake capacity of the composite toward Cu(II), Hg(II), Zn(II), and Ni(II) ions is 68.630, 50.942, 45.126, and 40.420 mg/g, respectively. The adsorption processes of the studied metal ions were spontaneous, chemical, and well described using the pseudo-second-order kinetic model and Langmuir equilibrium isotherm. The synthesized composite can be successfully regenerated and utilized various times in the removal of studied metal ions from aqueous media.

1. Introduction

Refining industrial effluents that are filled with heavy metal ions is considered one of the main challenges in the field of wastewater treatment owing to their extreme toxicity and the difficulty of degrading them by chemical or biological methods (Sharma et al., 2022; Malik et al., 2019; Mudhoo et al., 2012; Bashir et al., 2019). Heavy metal ions such as Ni (II), Cu(II), Zn(II), and Hg(II) cause much harms to the environment and humans because of their ability to accumulate in organisms through the food chain (Malik et al., 2017). A high concentration of Ni(II) ions in water, exceeding 0.1 mg/L causes many problems such as sensory disturbances, digestive disorders, high red blood cell count, and kidney failure (Osińska, 2017). A high concentration of Cu(II) ions in the water, exceeding 1.3 mg/L, causes many health problems for the kidneys, stomach, liver and causes anemia (Ashokkumar et al., 2016). A high concentration of Zn(II) ions in water, exceeding 5 mg/L, causes many problems such as stomach pain, nausea, headache, and diarrhea (Najafi, 2015). A high concentration of Hg(II) ions in water, exceeding 0.002 mg/L, cause many problems such as nervous system disorders, genetic disorders, skin rashes, fatigue, and headaches (Saad et al., 2013). Consequently, it is essential to research more cheaper and effective methods to remove heavy metal ions from effluents. The literature contains a lot of wastewater treatment methods for removing heavy metals such as liquid–liquid extraction, chemical precipitation, adsorption, membrane process, ion exchange, coagulation, and reverse osmosis (Amini-Fazl et al., 2021; Moja et al., 2021; Cerrahoğlu et al., 2017; Liu et al., 2022; Liang Liao et al., 2021; Efome et al., 2019; Ainscough et al., 2017). Adsorption has been widely relied upon as an effective method for removing a lot of heavy metal ions due to its high efficiency, ease, and simplicity (Abdelrahman et al., 2021; Abdelrahman et al., 2020; Abdelrahman and Hegazey, 2019; Abdelrahman and Hegazey, 2019; Abdelrahman et al., 2020; Abdelrahman and Subaihi, 2020; Hameed et al., 2020; Youssef et al., 2021). There are various reports about numerous adsorbents such as agricultural wastes, resins, activated carbon, organic/inorganic composites, zeolite, and bio-sorbent, which have been utilized for removing heavy metal ions from aqueous media (Sheng et al., 2004; Febrianto et al., 2009; Chang et al., 2007; Tan and Xiao, 2009; Shawabkeh, 2009; Denizli et al., 2003). Various metal organic frameworks (MOFs) have been identified as promising candidates for the adsorptive removal of heavy metal ions because of their unique features such as tunable porosity, large surface area, chemically stability, etc (Shamim et al., 2022). There are many products, have the ability to remove a lot of heavy metal ions, such as 2,4-Dinitrophenylhydrazine functionalized sodium dodecyl sulfate-coated magnetite nanoparticles, oxidized Multi-Walled Carbon Nanotubes, CeO_2 nanoparticles supported on $CuFe_2O_4$ nanofibers, chitosan, $TiO_2/SiO_2/Fe_3O_4$ nanoparticles, and $Fe_2O_3@SiO_2$ thin films (Sobhanardakani et al., 2015; Sobhanardakani et al., 2016; Talebzadeh et al., 2016; Sobhanardakani et al., 2016; Sobhanardakani and Zandipak, 2017; Sobhanardakani et al., 2018; Sobhanardakani and Zandipak, 2015). However, it is very important to synthesize new and effective adsorbents in simple ways. Our research group synthesizes a novel composite based on silica nanoparticles and Schiff base. Numerous Schiff bases can form chelates with a large number of heavy metal ions due to the strong affinity of metal ions toward N and O atoms. As a result, loading them onto solid supports such as silicon oxide to create novel composites can be efficiently used in the water pollution treatment. The paper's novel aspect stems from our research group's development of a new composite composed of silica nanoparticles and Schiff base. Firstly, silica nanoparticles, which contain silanol groups (Si-OH), reacted with (3-aminopropyl)tri methoxysilane. Then, the modified silica reacted with 1-hydroxy-2-acetonaphthone to form a novel Schiff base/silica composite. The synthesized composite was employed for the removal of Ni(II), Cu(II), Zn (II), and Hg(II) ions from aqueous media. Besides, 1-hydroxy-2-acetonaphthone was chosen as a material to modify the surface of silica because it contains two adjacent groups, OH and C=O, which are easily converted to C=N, making them have the ability to form stable hexagonal chelates with target metal ions and thus facilitate their efficient separation. Also, 1-hydroxy-2-acetonaphthone is easy to obtain due to its low price compared to the rest of the organic materials used for loading, such as dibenzoylmethane. Indeed, it is expected that this ligand can adsorb many ions, but for this research paper not to be too large, the ions of nickel, copper, zinc, and mercury were chosen as examples to prove the ability of the material to remove them, especially since these ions are highly toxic and dangerous.

2. Experimental

2.1. Materials and reagents

1-hydroxy-2-acetonaphthone ($C_{12}H_{10}O_2$), sodium metasilicate pentahydrate ($Na_2SiO_3{\cdot}5H_2O$), (3-aminopropyl)trimethoxysi lane ($C_6H_{17}NO_3Si$), cetyltrimethylammonium bromide ($C_{19}H_{42}BrN$), nitric acid (HNO_3), xylene (C_8H_{10}), ethanol (C_2H_6O), thiourea (CH_4N_2S), sulfuric acid (H_2SO_4), hydrochloric acid (HCl), nickel(II) chloride hexahydrate ($NiCl_2{\cdot}6H_2O$), sodium hydroxide (NaOH), potassium chloride (KCl), copper(II) chloride dihydrate ($CuCl_2{\cdot}2H_2O$), mercury (II) chloride ($HgCl_2$), zinc(II) chloride ($ZnCl_2$), and ethylenediaminetetraacetic acid disodium salt dihydrate ($C_{10}H_{16}N_2Na_4O_{10}$) were gotten from Sigma Aldrich Company (Purity = 99.99%) and utilized as received without further purification.

2.2. Synthesis of silica composite

Primarily, the SiO_2/(3-aminopropyl)trimethoxysilane sample was prepared according to the procedure illustrated by Khalifa et al. (2020). For obtaining silica nanoparticles; 12.00 g of cetyltrimethylammonium bromide was dissolved in 460 mL of distilled water. Then, 80.38 g of sodium metasilicate pentahydrate was added then the mixture was stirred for 30 min. Besides, the pH of the mixture was adjusted to 9 using 2 M of hydrochloric acid then the mixture was stirred for 4 hrs. The white gelatinous precipitate product was filtered, washed with distilled water, dried at 120 °C for 6 hrs, and calcined at 550 °C for 6 hrs. For obtaining SiO_2/(3-aminopropyl)trimethoxysilane, 2.00 g of the silica nanoparticles were added to a round flask containing 2.2 mL of (3-aminopropyl)trimethoxysilane and 30 mL toluene then the mixture was stirred under reflux at 120–140 °C for 24 hrs. The product was filtered, washed with ethanol, and dried at 50 °C for 24 hrs. After that, 2 g of the SiO_2/(3-aminopropyl)trimethoxysilane sample was mixed with 25 mL ethanolic solution including 2 g of 1-hydroxy-2-acetonaphthone then refluxed under stirring for one day in the presence of a few drops of concentrated H_2SO_4. Sulfuric acid helps to remove the water formed as a result of the reaction between the NH_2 and $C{=}O$ groups. Hence, it facilitates the process of Schiff base formation. Further, the produced SiO_2/Schiff base composite was filtered off, washed with ethanol, and dried under vacuum at 60 °C for one day.

2.3. Apparatus

The X-ray diffraction (XRD) patterns of the silica sample and their Schiff base composite were performed using an X-ray diffractometer (D8 Advance, Bruker, Billerica, Massachusetts, United States) where K_α Cu radiations with a wavelength equal to 0.15 nm were used. The Fourier transform (FT-IR) spectra of the silica sample and their Schiff base composite, were performed using Fourier transform infrared spectrophotometer (Nicolet, Waltham, Massachusetts, United States). The morphologies of the silica sample and their Schiff base composite were investigated using scanning electron microscopy (SEM, JEOL, SEM-JSM-5410LV, Akishima, Tokyo, Japan). The percent of carbon (C), hydrogen (H), and nitrogen (N) of the silica composite was estimated using CHN Elemental Analyzer (PerkinElmer, 2400, Waltham, United States). BET surface area, average pore radius, and total pore volume of the silica sample and their Schiff base composite were estimated using a nitrogen gas sorption analyzer (Quantachrome, NOVA, Boynton Beach, United States). Inductively Coupled Plasma Atomic Emission Spectrometry (ICP-AES) (PerkinElmer, 7500, Waltham, United States) was utilized for determining the concentration of studied metal ions in the solution.

2.4. Removal of Ni(II), Cu(II), Zn(II), and Hg(II) ions from aqueous media

In order to examine the effect of pH of metal ion solution, the pH values of 80 mL of 120 mg/L of Ni(II), Cu(II), Zn(II), or Hg(II) solutions were controlled to several values (pH = 2.5–6.5) before the addition of the composite utilizing 0.1 M NaOH or HCl. Afterward, 0.10 g of the composite is mixed with each Ni(II), Cu(II), Zn(II), or Hg(II) solution then the mixture was stirred for 200 min. In order to examine the effect of contact time, the pH values of 80 mL of 120 mg/L of Ni(II), Cu(II), Zn(II), or Hg(II) solutions were adjusted to 6.5 before the addition of the composites. Afterward, 0.10 g of the composite is mixed with each Ni(II), Cu(II), Zn(II), or Hg(II) solution then the mixture was stirred for several times (15–120 min).

In order to examine the effect of temperature, the pH values of 80 mL of 120 mg/L of Ni(II), Cu(II), Zn(II), or Hg(II) solutions were adjusted to 6.5 before the addition of the composite. Afterward, 0.10 g of the composite is mixed with each Ni(II), Cu(II), Zn(II), or Hg(II) solution then the mixture was stirred at several temperatures (298–328 K) for 90 min. In order to examine the effect of initial metal ion concentration, the pH values of 80 mL of 40–160 mg/L of Ni(II), Cu(II), Zn(II), or Hg(II) solutions were adjusted to 6.5 before the addition of the composite. Afterward, 0.10 g of the composite is mixed with each Ni(II), Cu(II), Zn(II), or Hg(II) solution then the mixture was stirred at 298 K for 90 min. After studying each of the aforementioned effects, the composite is separated utilizing centrifugation. Afterward, the residual concentration of Ni(II), Cu(II), Zn(II), or Hg(II) ions in the filtrate is determined using Inductively Coupled Plasma Atomic Emission Spectrometry (ICP-AES). The mass of the adsorbed Ni(II), Cu(II), Zn(II), or Hg(II) ions per gram of the composite (Q, mg/g) can be obtained utilizing Eq. (1).

$$Q = [C_i - C_e] \times \frac{V}{M} \tag{1}$$

The % removal (% R) of Ni(II), Cu(II), Zn(II), or Hg(II) ions can be obtained utilizing Eq. (2).

$$\%R = \frac{C_i - C_e}{C_i} \times 100 \tag{2}$$

where, C_i (mg/L) represents the initial concentration of Ni(II), Cu(II), Zn(II), or Hg(II) ions while C_e (mg/L) represents the final concentration of Ni(II), Cu(II), Zn(II), or Hg(II) ions. Furthermore, V (L) represents the volume of Ni(II), Cu(II), Zn(II), or Hg(II) solution while M (g) represents the mass used of the composite. In order to examine the influence of desorption, 0.10 g of the composite was stirred with 80 mL of 120 mg/L of Ni(II), Cu(II), Zn(II), or Hg(II) solution (pH = 6.5) for 90 min. Furthermore, the composite was separated utilizing centrifugation then carefully washed with distilled water. The composite which loaded with Ni(II), Cu(II), Zn(II), or Hg(II) ions was then stirred for 50 min with 40 mL of 0.45 M of some desorbing solutions (hydrochloric acid, nitric acid, EDTA disodium salt, and thiourea). In order to examine the reusability experiments for four cycles of adsorption/desorption, 0.10 g of the regenerated composite was stirred with 80 mL of 120 mg/L of Ni(II), Cu(II), Zn(II), or Hg(II) solution (pH = 6.5) for 90 min. It is noteworthy that 0.45 M of EDTA disodium salt is utilized for regenerating the composite after each cycle. The % desorption (% D) can be obtained utilizing Eq. (3).

$$\%D = \frac{100 C_d V_d}{(C_i - C_e)V} \tag{3}$$

where, C_d (mg/L) represents the concentration of Ni(II), Cu(II), Zn(II), or Hg(II) ions that exist in the desorption solution while V_d (L) represents the volume of desorbing solution.

The point of zero charge (pH_{PZC}) of the composite can be obtained as clarified by Khalifa et al. (Khalifa et al., 2020) as the following; the initial pH value of 0.025 M of potassium chloride solutions was controlled to several values from 2 to 12 utilizing 0.1 M NaOH or HCl. Afterward, 0.10 g of the composite was mixed with each potassium chloride solution then the mixture was stirred for 8 hrs. Furthermore, the composite was separated utilizing centrifugation then the final pH value (pH_{final}) of the filtrates was determined. pH_{final} values were plotted against $pH_{initial}$ values. The pH_{pzc} is the pH_{final} level where a typical plateau was gotten (Khalifa et al., 2020). The effect of interference between each of the Cu(II), Hg(II), Zn(II), or Ni(II) metals ions and interference metal ions such as Co(II), Fe(III), Pb(II), and Al(III) were studied as follows: 0.1 g of the synthesized composite was mixed together with 80 mL of 120 mg/L of metal ions (Cu(II), Hg (II), Zn(II), or Ni(II)) solution (pH = 6.5) which contains Co(II), Fe(III), Pb(II), or Al(III) with different concentrations (50, 80, and 100 mg/L). Then, the mixture was stirred at 298 K for 90 min.

3. Results and discussion

3.1. Characterization of the composite

Fig. 1A-B illustrates the X-ray diffraction patterns of the silica and their Schiff base composite, respectively. Also, the results confirmed that the synthesized silica is cristobalite that has a tetragonal system as consistent with JCPDS card No. 00-039-1425 (Xue et al., 2015). The average crystallite size of the formed silica is 45.63 nm. The considerable reduction at 2θ = 21.9° in the intensity of the XRD peak of the composite is owing to the formation of the Schiff base as clarified in Scheme 1. Fig. 2A-B illustrates the FT-IR spectra of the silica and their Schiff base composite, respectively. Six bands for silica are observed at 466, 620, 790, 1069, 1618, and 3445 cm^{-1}.

The observed band at 466 cm^{-1} is owing to the bending vibrations of Oxygen–Silicon–Oxygen. The observed bands at 620 and 790 cm^{-1} are owing to the symmetrical stretching vibrations of Silicon–Oxygen–Silicon. The observed band at 1069 cm^{-1} is owing to the asymmetrical stretching vibrations of Silicon–Oxygen–Silicon. The observed bands at 3445 and 1618 cm^{-1} are owing to the stretching and bending vibrations of OH (Correcher et al., 2009). In the case of the composite, the bands of silica are observed at 476, 619, 790, 1090, 1604, and 3440 cm^{-1}. The shift in the positions of these IR peaks confirmed that the Schiff base has undergone a chemical change with the silica. The observed bands at 3440 and 1604 cm^{-1} are owing to the stretching and bending vibrations of OH and/or C=N, respectively. The observed bands at 3005 and 2942 cm^{-1} are owing to the stretching vibrations of CH aromatic and CH aliphatic, respectively. The observed bands at 1437, 1476, and 1510 cm^{-1} are owing to the stretching vibrations of C=C aromatic. The observed band at 1373 cm^{-1} is owing to the bending vibrations of CH. The observed bands at 840 and 920 cm^{-1} are owing to the out-of-plane bending vibrations of CH aromatic (Xu and Braterman, 2003). Elemental analysis of the composite demonstrated that the % C, % H, and % N are 15.26, 3.24, and 1.65 %, respectively. Consequently, the presence of nitrogen and carbon proves the effective loading of the Schiff base on the silica as displayed in Scheme 1. Fig. 3A-B illustrates the FE-SEM images of the silica and their Schiff base composite, respectively. The results confirmed that the silica includes irregular shapes whereas the composite possesses a flaky surface owing to the formation of the Schiff base. Fig. 4A-B illustrates the N_2 adsorption/desorption isotherms of the silica and their Schiff base composite, respectively. The data demonstrated that the gotten isotherms belong to type IV (Abdelrahman et al., 2019). Total pore vol-

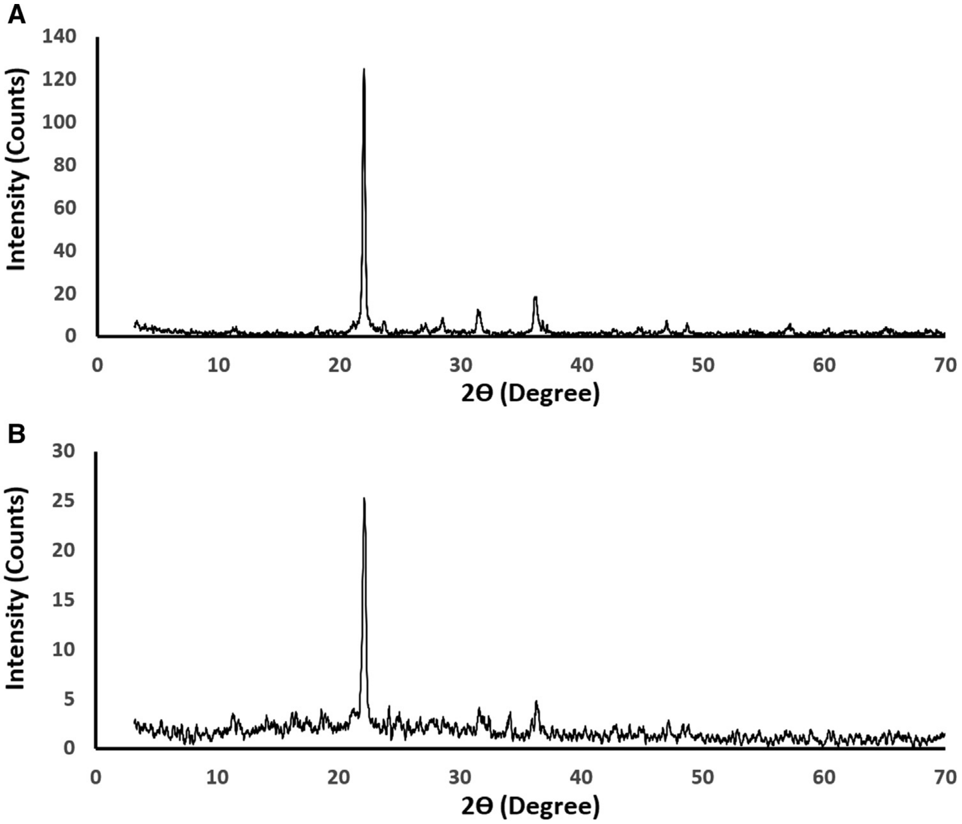

Fig. 1 The X-ray diffraction patterns of the silica (A) and their Schiff base composite (B).

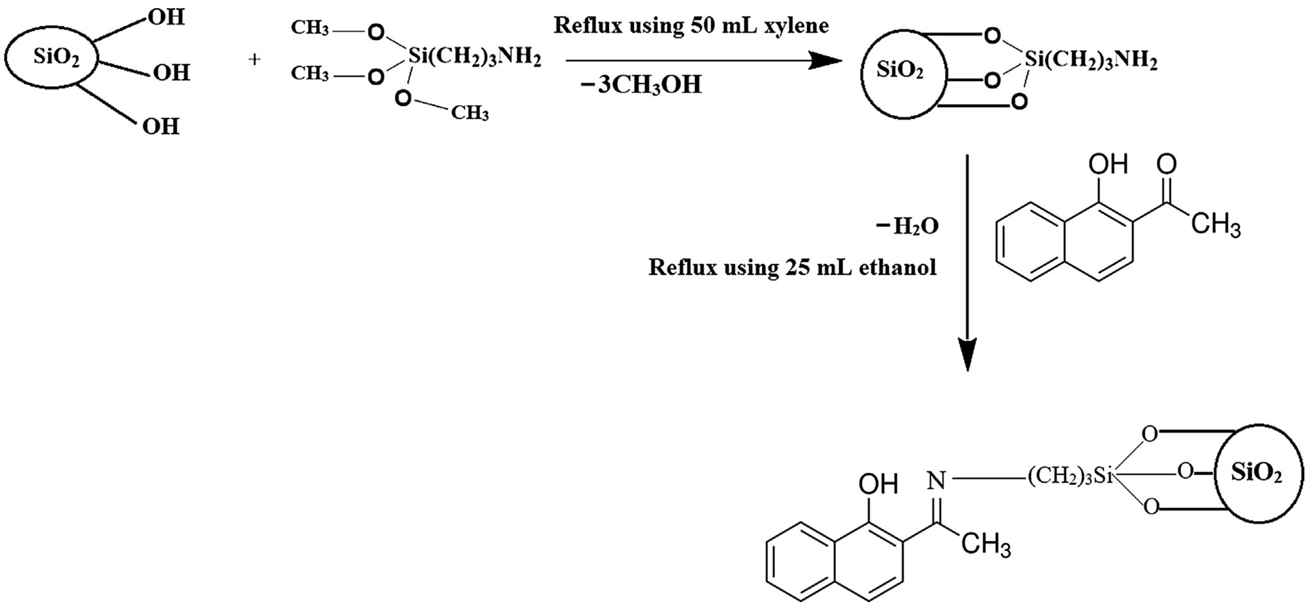

Scheme 1 The synthetic steps of the composite.

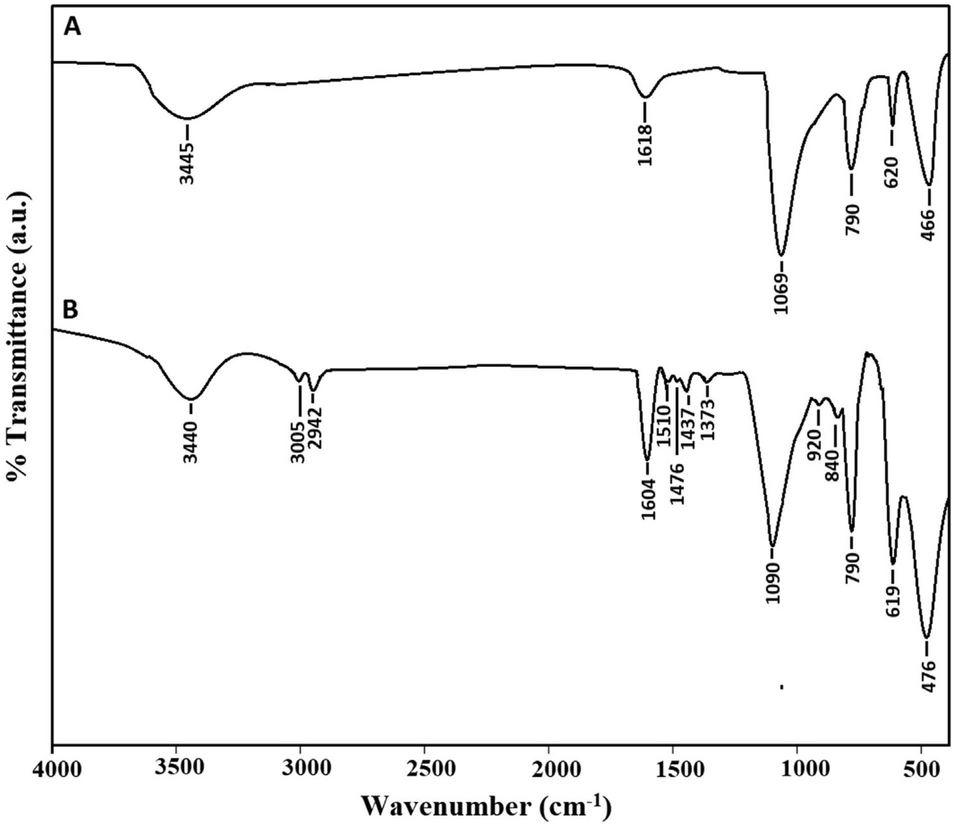

Fig. 2 The FT-IR spectra of the silica (A) and their Schiff base composite (B).

ume, BET surface area, and average pore size were presented in Table 1. The BET surface area and total pore volume of the composite were reduced because the formed Schiff base blocks the pores of silica. Therefore, this analysis proves the effective loading of the Schiff base on the silica as presented in Scheme 1.

3.2. Removal of Ni(II), Cu(II), Zn(II), and Hg(II) ions from aqueous media

3.2.1. Effect of pH

Fig. 5A-B illustrates the effect of pH of the studied metal ion solution on % R and Q (mg/g), respectively. The results con-

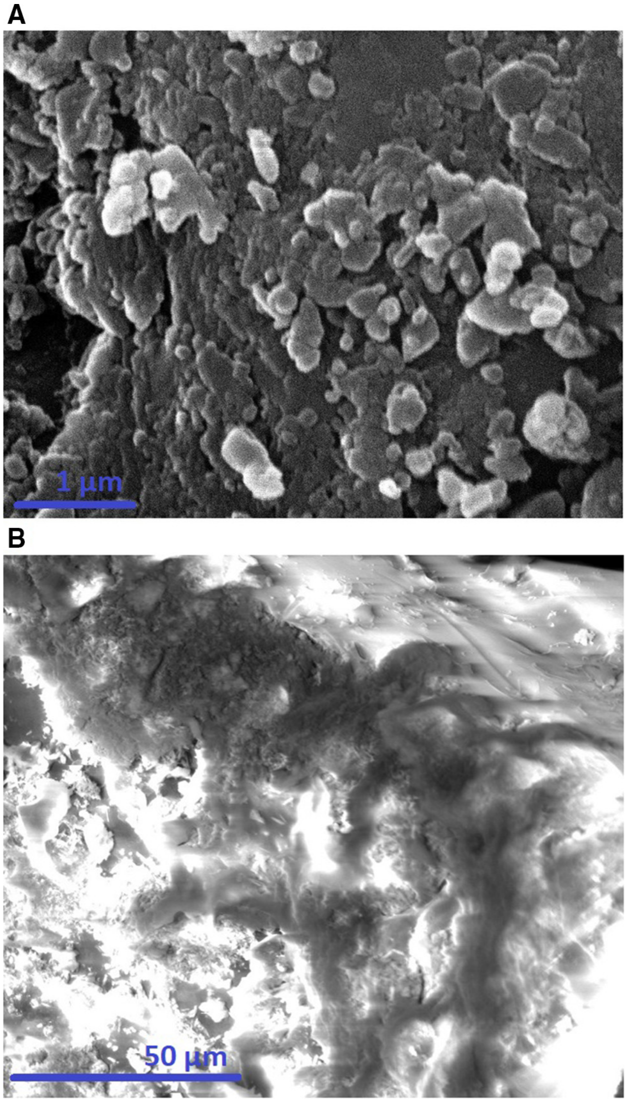

Fig. 3 The FE-SEM images of the silica (A) and their Schiff base composite (B).

firmed that % R or Q increases with the increases in the pH to attain a maximum at pH 6.5. At pH = 1.5, Hg(II) ions exhibit abnormal behavior because they can form anions in chloride media at low pH ($HgCl_3^-$) and electrostatically connect with the protonated sides of the ligand. % R of Cu(II), Hg(II), Zn(II), and Ni(II) ions at pH = 6.5 is 62.02, 47.44, 44.88, and 35.83, respectively. Q of the composite toward of Cu(II), Hg(II), Zn(II), and Ni(II) ions at pH = 6.5 is 59.54, 45.54, 43.09, and 34.40 mg/g, respectively. Fig. 5C illustrates the plot of pH_{final} against $pH_{initial}$ for some potassium chloride solutions. The results confirmed that the point of zero charge of the composite is 3.01. If the pH of the Cu(II), Hg(II), Zn(II), or Ni(II) solution is less than 3.01, the composite is positively charged because it is surrounded by positive hydrogen ions that repel studied metal ions and therefore % R or Q decreases. In contrast, if the pH of the Cu(II), Hg(II), Zn (II), or Ni(II) is higher than 3.01, the composite is negatively charged because it is surrounded by negative hydroxide ions that attract studied metal ions and therefore, % R or Q increases (Khalifa et al., 2020).

3.2.2. *Effect of contact time*

Fig. 6A-B illustrates the effect of contact time of the studied metal ion solution on % R and Q (mg/g), respectively. The results confirmed that % R or Q increases with the increases in the time to attain a maximum at time = 90 min. Q or % R was not changed when the contact time go beyond 90 min owing to the saturation of the active sites. % R of Cu(II), Hg(II), Zn(II), and Ni(II) ions at time = 90 min is 62.50, 47.50, 45.00, and 35.83, respectively. Also, Q of the composite toward Cu(II), Hg(II), Zn(II), and Ni(II) ions at time = 90 min is 60.00, 45.60, 43.20, and 34.40 mg/g, respectively.

The results of contact time were investigated by two kinetic models, namely: pseudo-second-order (Eq. (4)) and pseudo-first-order (Eq. (5)) (Abdelrahman et al., 2021; Abdelrahman et al., 2020; Abdelrahman and Hegazey, 2019; Abdelrahman and Hegazey, 2019).

$$\frac{t}{Q_t} = \frac{1}{K_2 Q_e^2} + \frac{1}{Q_e} t \tag{4}$$

$$\log(Q_e - Q_t) = logQ_e - \frac{K_1}{2.303} t \tag{5}$$

where, Q_e (mg/g) represents the uptake capacity of the composite toward studied metal ions at the equilibrium while Q_t (mg/g) represents the uptake capacity of the composite toward studied metal ions at the contact time t. K_1 (1/min) represents the rate constant of the pseudo-first-order model while K_2 (g/mg.min) represents the rate constant of the pseudo-second-order model. Fig. 7A-B illustrates the pseudo-first-order and pseudo-second-order models, respectively. The data demonstrated that the correlation coefficients (R^2) of the pseudo-first-order model are smaller than those of the pseudo-second-order model as displayed in Table 2. Besides, Q_e, which was gotten from the pseudo-second-order, is consistent with the experimental uptake capacity more than that of the pseudo-first-order. Therefore, the kinetic results were well described using the pseudo-second-order model than the pseudo-first-order model. Nonlinear kinetic models were studied as described by Altowayti et al. (Figures omitted for brevity). The R^2 value derived from the nonlinear plot is much smaller than that derived from the linear model. The results of this study showed that the nonlinear method is a good way to show the kinetic data (Altowayti et al., 2021).

3.2.3. *Effect of temperature*

Fig. 8A-B illustrates the effect of temperature of the studied metal ion solution on % R and Q (mg/g), respectively. The results confirmed that % R or Q decreases with the increases in the temperature to attain a minimum at temperature = 328 K. % R of Cu(II), Hg(II), Zn(II), and Ni(II) ions at temperature = 328 K is 22.50, 15.00, 10.83, and 6.08, respectively. Also, Q of the composite toward Cu(II), Hg(II), Zn(II), and Ni(II) ions at temperature = 328 K is 21.60, 14.40, 10.40, and 5.84 mg/g, respectively. Hence, the optimum temperature is 298 K. The thermodynamic parameters such as a change in enthalpy (ΔH°), change in the entropy (ΔS°), and change in free energy (ΔG°) were calculated utilizing Eqs. (6)&(7) (Abdelrahman et al., 2021; Abdelrahman et al., 2020; Abdelrahman and Hegazey, 2019; Abdelrahman and Hegazey, 2019).

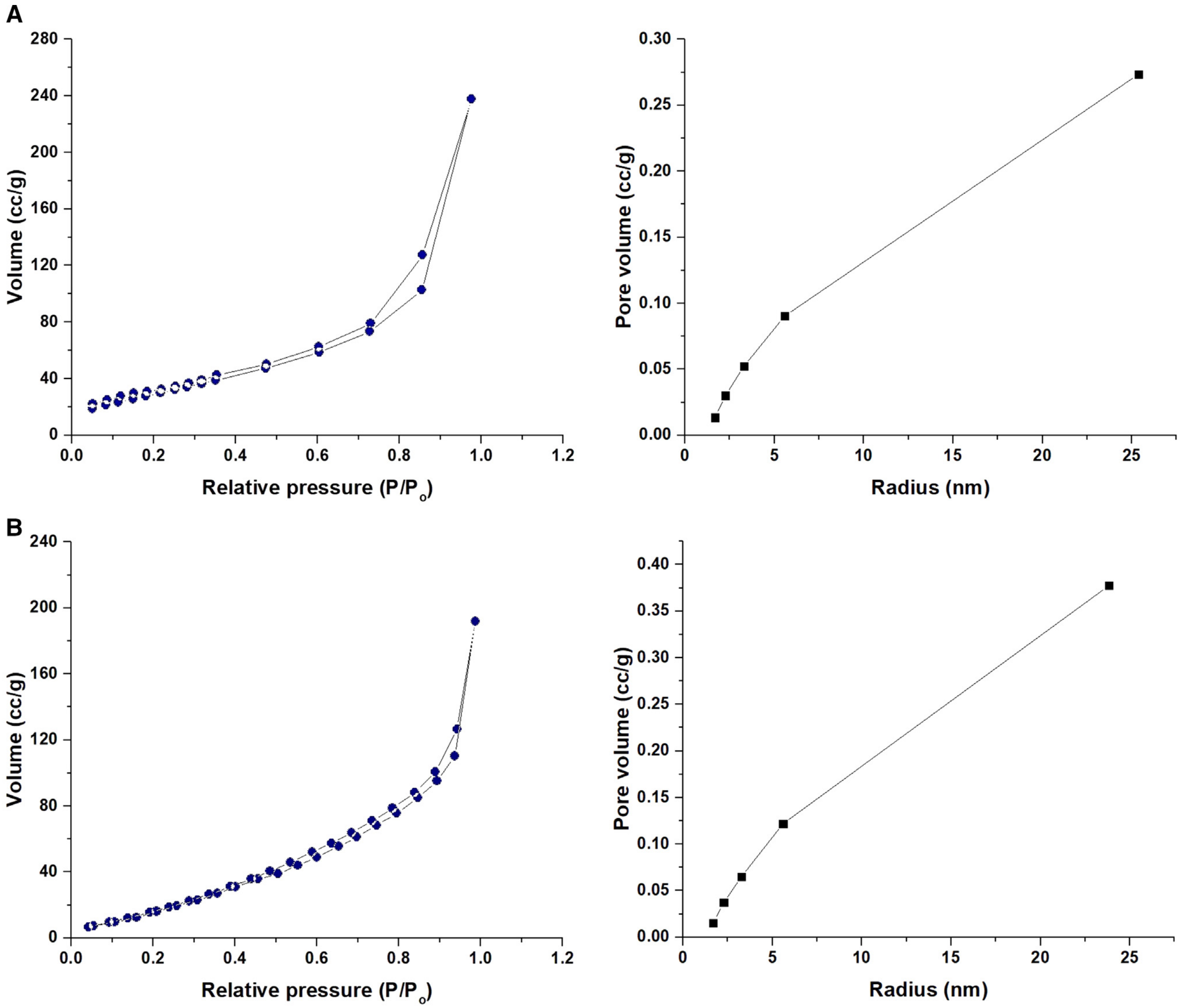

Fig. 4 The N_2 adsorption/desorption isotherms of the silica (A) and their Schiff base composite (B).

Table 1 The surface textures of the silica and their Schiff base composite.

Sample	BET surface area (m^2/g)	Total pore volume (cc/g)	Average pore size (nm)
SiO_2	110.142	0.340	6. 253
Composite	89.431	0.172	3.067

$$lnK_d = \frac{\Delta S^o}{R} - \frac{\Delta H^o}{RT} \quad (6)$$

$$\Delta G^o = \Delta H^o - T\Delta S^o \quad (7)$$

where, T (Kelvin) represents the adsorption temperature while K_d (L/g) represents the distribution constant. Also, R (kJ/mol kelvin) represents a gas constant. The distribution constant (K_d) was calculated utilizing Eq. (8) (Abdelrahman et al., 2021; Abdelrahman et al., 2020; Abdelrahman and Hegazey, 2019; Abdelrahman and Hegazey, 2019).

$$K_d = \frac{Q_e}{C_e} \quad (8)$$

Fig. 8C illustrates the plot of $\ln K_d$ against temperature. The thermodynamic parameters are scheduled in Table 3. The data confirmed that the uptake of Cu(II), Hg(II), Zn(II), or Ni(II) ions using composite is chemical because the value of enthalpy is above 40 kJ/mol (Khalifa et al., 2020). Besides, the uptake of Cu(II), Hg(II), Zn(II), or Ni(II) ions using composite is exothermic due to the negative sign of enthalpy. The synthesized composite can form chelates with Cu(II), Hg(II), Zn

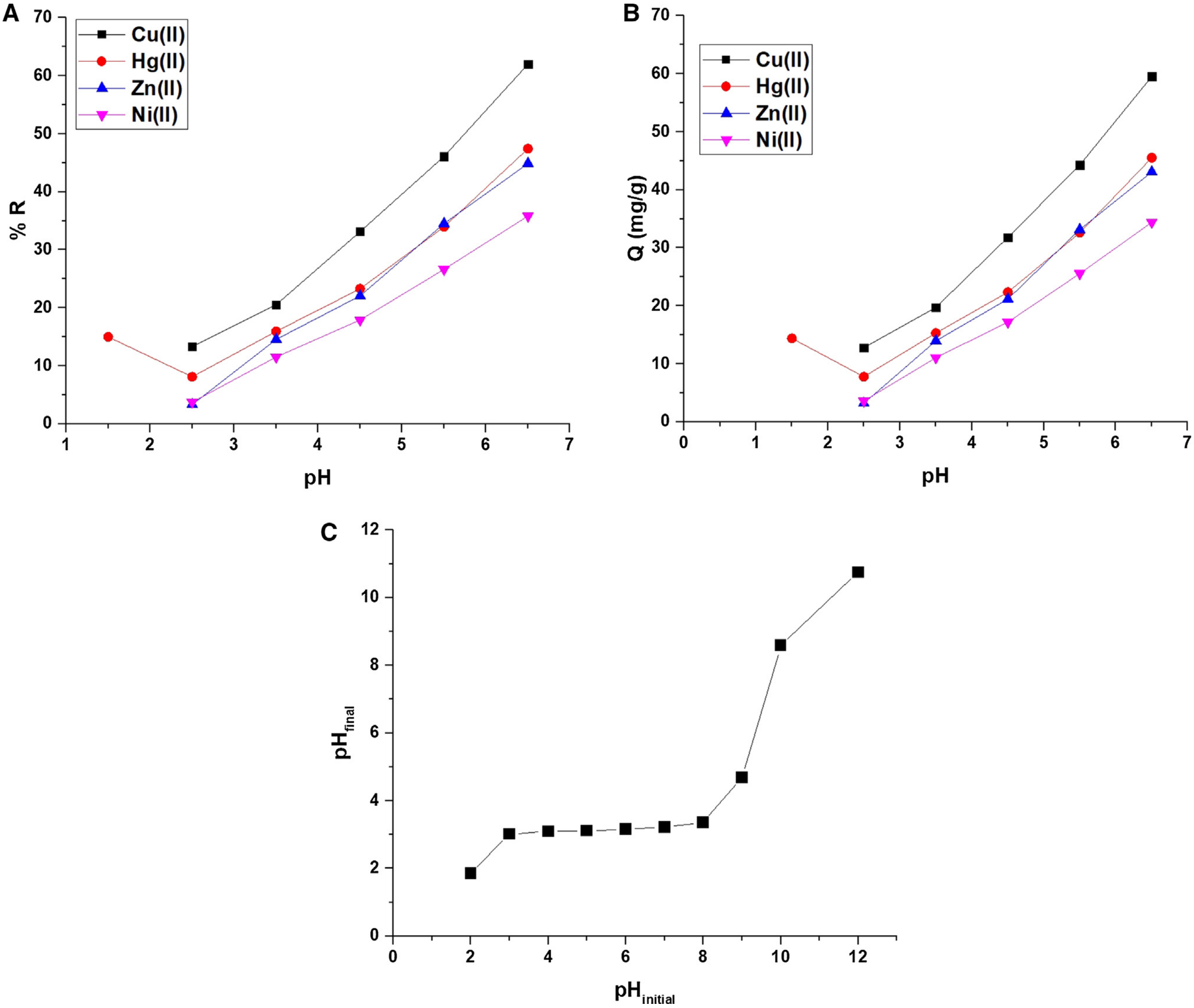

Fig. 5 The effect of pH of the studied metal ion solution on % R (A) and Q B).

(II), or Ni(II) ions as shown in Scheme 2. Moreover, the uptake of Cu(II), Hg(II), Zn(II), or Ni(II) ions using composite is spontaneous due to the negative sign of free energy. Additionally, the uptake of Cu(II), Hg(II), Zn(II), or Ni(II) ions takes place in a disordered approach at the solution boundary/composite owing to the positive sign of entropy.

3.2.4. Effect of concentration

Fig. 9A-B illustrates the effect of concentration of the studied metal ion solution on % R and Q (mg/g), respectively. The results confirmed that % R decreases while Q increases with the increases in the concentration. % R of Cu(II), Hg(II), Zn (II), and Ni(II) ions at concentration = 160 mg/L is 52.50, 38.13, 34.38, and 30.00, respectively. Also, Q of the composite toward Cu(II), Hg(II), Zn(II), and Ni(II) ions at concentration = 160 mg/L is 67.20, 48.80, 44.00, and 38.40 mg/g, respectively. The results of concentration were investigated using two equilibrium isotherms, namely: Freundlich (Eq. (9)) and Langmuir (Eq. (10)) (Abdelrahman et al., 2021; Abdelrahman et al., 2020; Abdelrahman and Hegazey, 2019; Abdelrahman and Hegazey, 2019).

$$lnQ_e = lnK_3 + \frac{1}{n} lnC_e \tag{9}$$

$$\frac{C_e}{Q_e} = \frac{1}{K_4 Q_m} + \frac{C_e}{Q_m} \tag{10}$$

where, Q_m (mg/g) represents the maximum uptake capacity of the composite. K_4 (L/mg) represents the Langmuir constant while K_3 (mg/g)(L/mg)$^{1/n}$) represents the Freundlich constant. 1/n represents the heterogeneity constant. The Q_m can be determined from the Freundlich isotherm utilizing Eq. (11) (Abdelrahman et al., 2021; Abdelrahman et al., 2020; Abdelrahman and Hegazey, 2019; Abdelrahman and Hegazey, 2019).

$$Q_m = K_3\left(C_i^{1/n}\right) \tag{11}$$

Fig. 10A-B illustrates the Langmuir and Freundlich isotherms, respectively. The data demonstrated that the correlation coefficients (R^2) of the Freundlich isotherm are smaller than those of Langmuir as clarified in Table 4. Therefore, the equilibrium results were well described using the Langmuir isotherm than the Freundlich isotherm. Nonlinear equilibrium

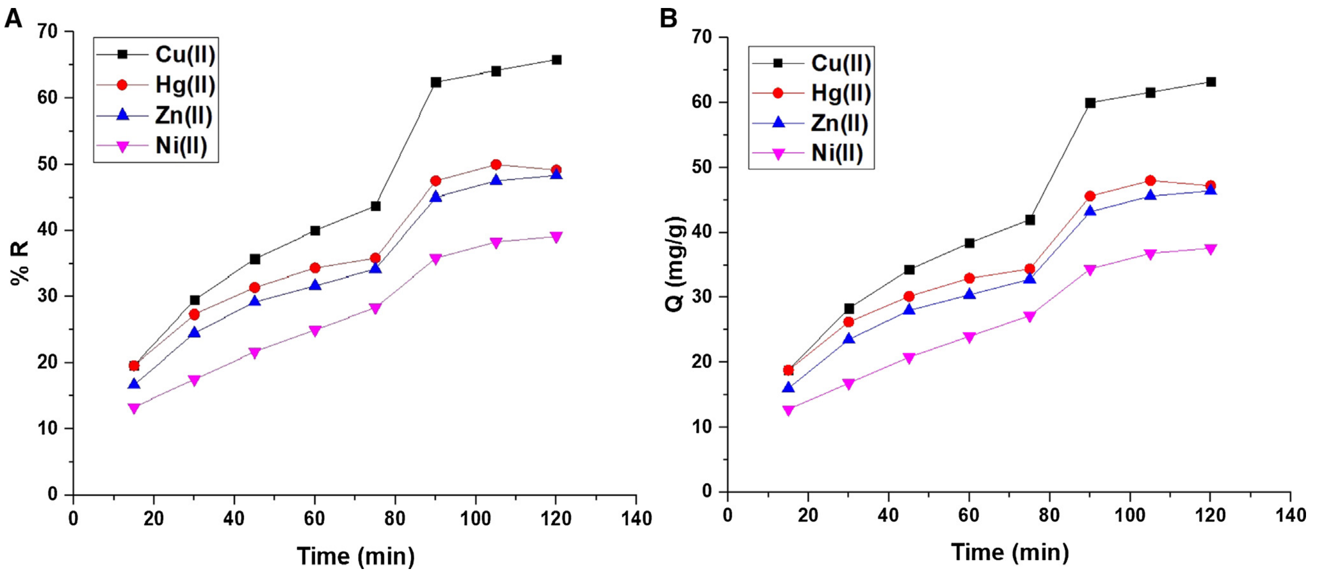

Fig. 6 The effect of contact time of the studied metal ion solution on % R (A) and Q B).

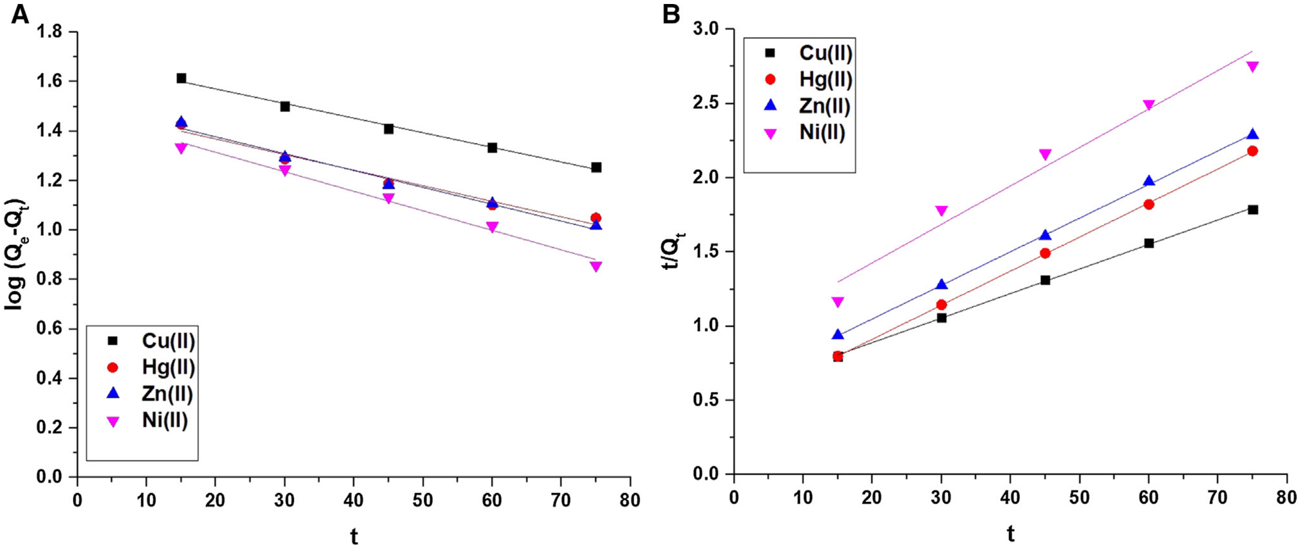

Fig. 7 The pseudo-first-order (A) and pseudo-second-order (B) models.

Table 2 Kinetic constants for the removal of Cu(II), Hg(II), Zn(II), and Ni(II) ions using the synthesized composite.

Metal ion	Pseudo first order				Pseudo second order			
	Q_e (mg/g)		K_1 (1/min)	R^2	Q_e (mg/g)		K_2 (g/mg.min)	R^2
	Calculated	Experimental			Calculated	Experimental		
Cu(II)	48.84	59.54	0.014	0.990	60.49	59.54	0.00048	0.999
Hg(II)	31.19	45.54	0.015	0.963	43.59	45.54	0.00115	0.999
Zn(II)	32.62	43.09	0.016	0.979	44.42	43.09	0.00086	0.999
Ni(II)	29.67	34.40	0.018	0.984	38.61	34.40	0.00073	0.995

isotherms were studied as described by Altowayti et al. (Figures omitted for brevity). The R^2 value derived from the nonlinear plot is much smaller than that derived from the linear isotherm. The results of this study showed that the nonlinear method is a good way to show the equilibrium data (Altowayti et al., 2021). The maximum uptake capacity of the composite toward Cu(II), Hg(II), Zn(II), or Ni(II) ions is 68.630, 50.942, 45.126, and 40.420 mg/g, respectively. The

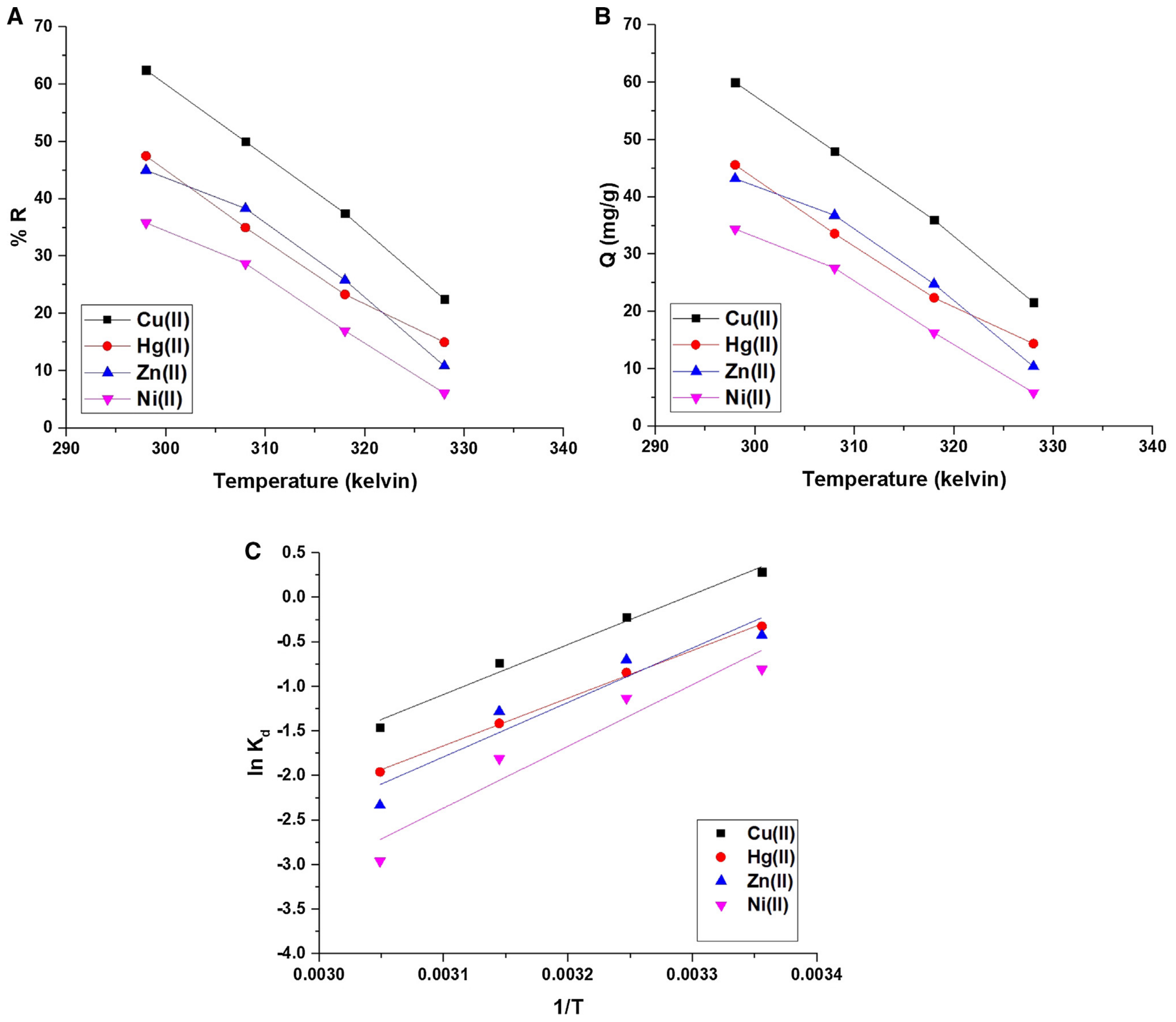

Fig. 8 The effect of temperature of the studied metal ion solution on % R (A) and Q B). Fig. 8**C.** The plot of $\ln K_d$ against temperature.

Table 3 Thermodynamic parameters for the removal of Cu(II), Hg(II), Zn(II), and Ni(II) ions using the synthesized composite.

Metal ion	ΔG^o (KJ/mol)				ΔS^o (KJ/molK)	ΔH^o (KJ/mol)
	Temperature (Kelvin)					
	298	308	318	328		
Cu(II)	−92.887	−94.431	−95.975	−97.519	0.154	−46.875
Hg(II)	−90.117	−91.641	−93.166	−94.690	0.152	−44.89
Zn(II)	−102.662	−104.394	−106.126	−107.858	0.173	−51.049
Ni(II)	−117.241	−119.232	−121.224	−123.216	0.199	−57.884

maximum uptake capacity of the unmodified silica toward Cu (II), Hg(II), Zn(II), or Ni(II) ions is 5.25, 4.26, 2.83, and 2.24 mg/g, respectively. These values are weak for unmodified silica because the adsorption is physical in the absence of a Schiff base. On the contrary, the high adsorption capacity values in the case of the composite are due to the presence of a Schiff base, which has the ability to the chemical adsorption through the formation of chelates with studied metal ions. A comparison study was carried out between the uptake capacity of the synthesized composite with that of other adsorbents such as iron oxide/chitosan composite, graft copolymer, montmorillonite, modified zeolite with 4-(3-triethoxysilylpropyl).

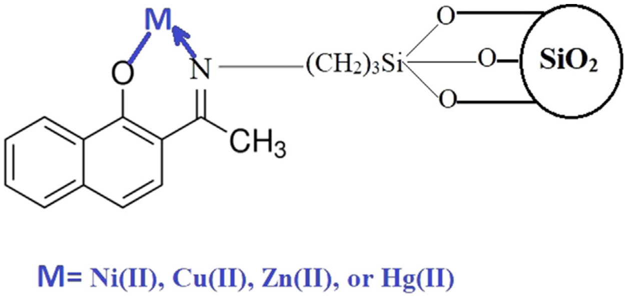

Scheme 2 The adsorption mechanism.

thiosemicarbazide, guanyl-modified cellulose, and mercaptotriazole-functionalized nickel-zinc ferrite microspheres as clarified in Table 5 (Shah et al., 2021; Adamovich et al., 2021; Chen et al., 2015; Kenawy et al., 2018; Ma et al., 2021; Monier and Abdel-Latif, 2012). Noticeably, the synthesized composite reaches higher Q values (mg/g) compared to the materials presented in Table 5. This can be explained because the loaded Schiff base can form chelates with studied metal ions due to the strong affinity of metal ions toward N and O atoms as shown in Scheme 2.

3.2.5. *Effect of desorption and reusability*

Fig. 11 illustrates the plot of % D against some desorbing solutions. The used desorbing solutions are 0.45 M of hydrochloric acid, nitric acid, thiourea, and EDTA disodium salt. The data demonstrated that 0.45 M of EDTA disodium salt is the suitable desorbing solution that needed for the maximum recovery of the studied metal ions from the synthesized composite. EDTA is the head member of the family of ligands.

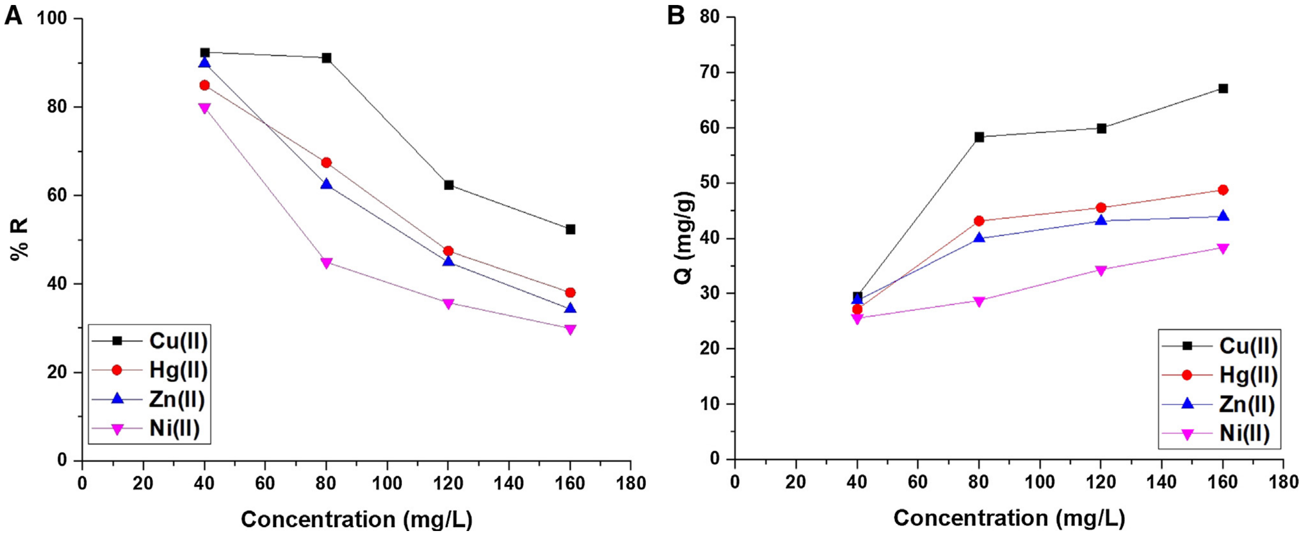

Fig. 9 The effect of concentration of the studied metal ion solution on % R (A) and Q B).

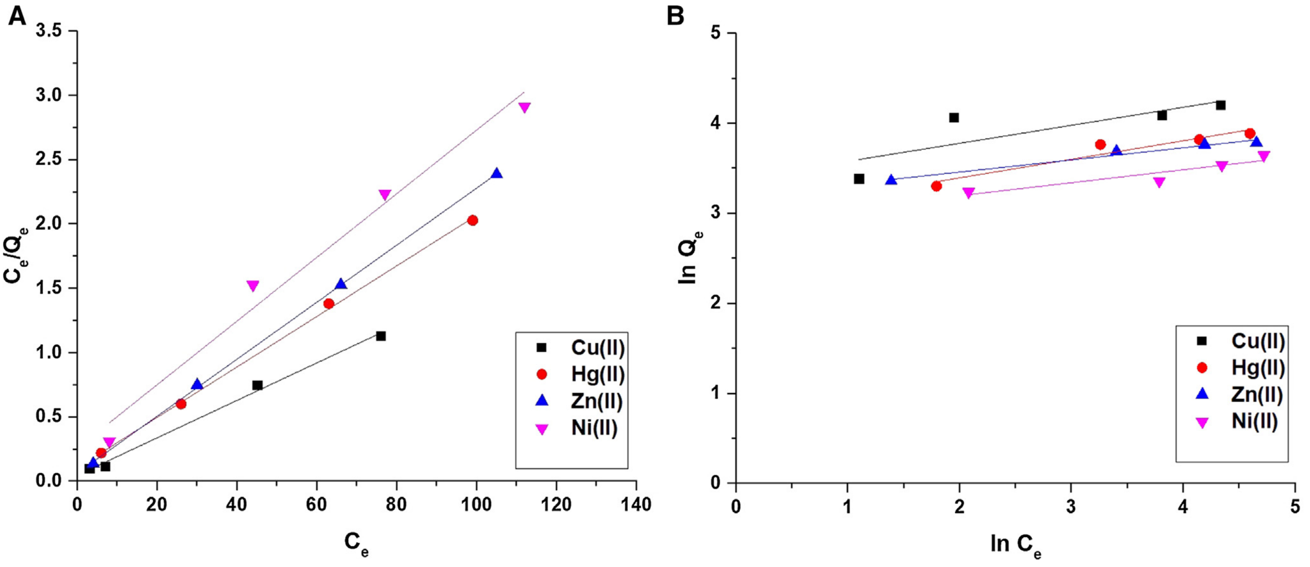

Fig. 10 The Langmuir (A) and Freundlich (B) isotherms.

Table 4 Equilibrium constants for the removal of Cu(II), Hg(II), Zn(II), and Ni(II) ions using the synthesized composite.

Metal ion	Langmuir			Freundlich		
	Q_m (mg/g)	K_4 (L/mg)	R^2	Q_m (mg/g)	K_3 (mg/g)(L/mg)$^{1/n}$	R^2
Cu(II)	68.630	0.301	0.993	76.526	29.379	0.505
Hg(II)	50.942	0.185	0.998	53.005	19.765	0.880
Zn(II)	45.126	0.339	0.999	46.336	24.294	0.959
Ni(II)	40.420	0.096	0.971	36.570	18.362	0.794

Table 5 A comparative study between the adsorption capacity of the composite with other materials.

Adsorbent	Q (mg/g) toward Cu(II) ions	Q (mg/g) toward Hg(II) ions	Q (mg/g) toward Zn(II) ions	Q (mg/g) toward Ni(II) ions	Ref
Iron oxide/chitosan composite	–	–	–	1.140	(Shah et al., 2021)
Graft copolymer of chitosan with 2-acrylamido-2-methyl-1-propanesulfonic acid	–	–	–	32.74	(Shah et al., 2021)
Zeolite modified with 4-(3-triethoxysilylpropyl) thiosemicarbazide	29.50	–	–	16.60	(Adamovich et al., 2021)
Montmorillonite	7.500	–	9.664	–	(Chen et al., 2015)
Guanyl-modified cellulose	83.78	48.00	68.52	–	(Kenawy et al., 2018)
Mercaptotriazole-functionalized nickel-zinc ferrite microspheres	–	66.25	–	–	(Ma et al., 2021)
Modified magnetic chitosan	–	–	35.30	–	(Monier and Abdel-Latif, 2012)
SiO_2/Schiff base composite	68.630	50.942	45.126	40.420	**This study**

Table 6 The effect of interference ions on the % removal of Cu(II), Hg(II), Zn(II), and Ni(II) ions using the synthesized composite.

Interference metal ion		% R			
Type	Concentration (mg/L)	Cu(II)	Hg(II)	Zn(II)	Ni(II)
Co(II)	0	62.02	47.44	44.88	35.83
	50	60.14	46.04	43.78	34.16
	80	50.25	38.03	36.04	27.97
	100	48.23	35.00	34.75	25.08
Fe(III)	0	62.02	47.44	44.88	35.83
	50	59.06	45.00	42.03	33.15
	80	51.12	35.75	35.12	30.03
	100	45.87	33.03	33.09	28.16
Pb(II)	0	62.02	47.44	44.88	35.83
	50	60.13	46.01	43.00	33.00
	80	56.05	39.12	37.06	26.37
	100	50.32	36.43	34.25	24.95
Al(III)	0	62.02	47.44	44.88	35.83
	50	61.06	46.56	42.97	31.14
	80	50.75	38.07	39.03	28.07
	100	47.98	36.16	37.35	25.86

EDTA is a hexadentate ligand forming highly stable complexes with Cu(II), Hg(II), Zn(II), and Ni(II) ions in an aqueous solution. So, it has the affinity to uptake these metal ions from the composite surface (Valle et al., 2015; Elgueta et al., 2016). Fig. 12 illustrates the plot of % R against the adsorption/desorption cycle number. The slight reduction in % R proves that the synthesized composite can be effectively utilized various times in the uptake of Cu(II), Hg(II), Zn(II), and Ni(II) ions from aqueous media.

3.2.6. Effect of interference

To examine the effect of several ions such as Co(II), Fe(III), Pb (II), and Al(III) on the extraction efficacy of Cu(II), Hg(II), Zn, and Ni(II) ions operating the present composite, the potential interference ion was added at several concentrations to a 80 mL solution containing 120 mg/L of the examined metal ion individually. Then, the adsorption procedure was carried out exactly as stated in the experimental part. Table 6

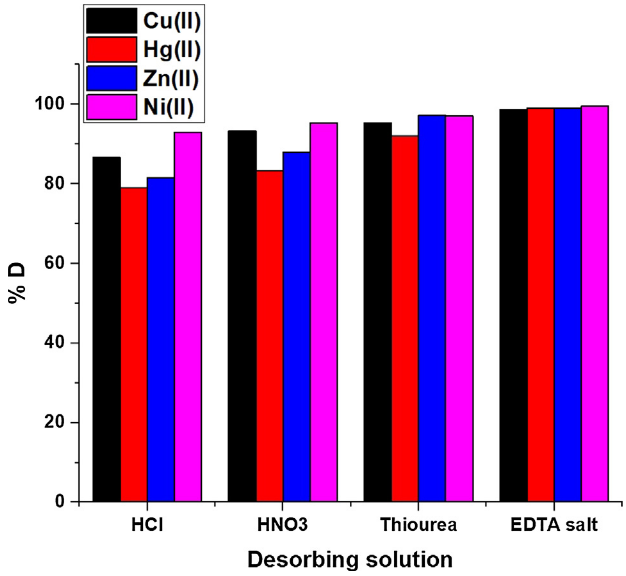

Fig. 11 The plot of % D against some desorbing solutions.

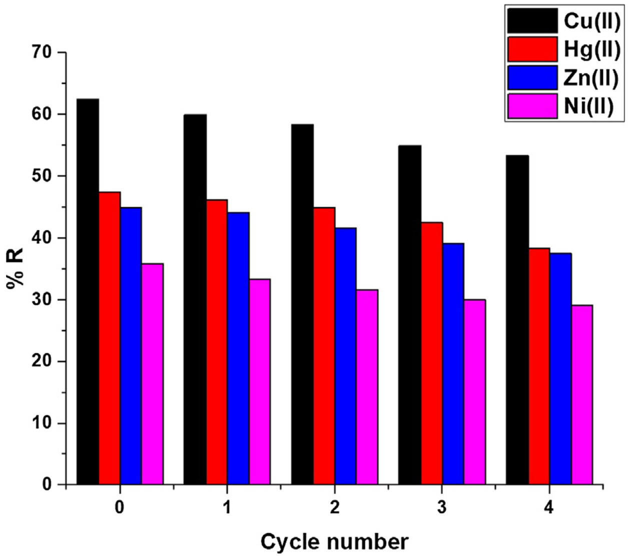

Fig. 12 The plot of % R against the cycle number.

represents the effect of the concentration of interference ions on % R of studied metal ions. The interfering ions were Co (II), Fe(III), Pb(II), and Al(III). The obtained results indicate that there is a slight decrease in the value of % R of studied metal ions in the presence of 50-fold excess of the interfering metal ion concentration. Also, there is a significant decrease in the value of % R of studied metal ions when the concentration of the interfering metal ion equals 80 or100 fold excess.

4. Conclusions

A novel composite was synthesized by modifying silica nanoparticles with 1-hydroxy-2-acetonaphthone. The synthesized composite was characterized using several tools such as XRD, FT-IR, FE-SEM, N_2 adsorption/desorption analyzer, and CHN analyzer. The synthesized composite was employed for the efficient removal of Ni(II), Cu(II), Zn(II), and Hg(II) ions from aqueous media. The maximum uptake capacity of the composite toward Cu(II), Hg(II), Zn(II), or Ni(II) ions is 68.630, 50.942, 45.126, and 40.420 mg/g, respectively. The results confirmed that the maximum % removal of studied metal ions was achieved at pH = 6.5, contact time = 90 min, and adsorption temperature = 298 K.

Declaration of Competing Interest

The authors declare that they have no known competing financial interests or personal relationships that could have appeared to influence the work reported in this paper.

Acknowledgements

The authors are grateful to Princess Nourah Bint Abdulrahman University, Riyadh, Saudi Arabia for funding this work through Researches Supporting Project number (PNURSP2022R35). The authors are grateful to the Deanship of Scientific Research, King Saud University for funding through Vice Deanship of Scientific Research Chairs.

References

Abdelrahman, E.A., Hegazey, R.M., El-Azabawy, R.E., 2019. Efficient removal of methylene blue dye from aqueous media using Fe/Si, Cr/Si, Ni/Si, and Zn/Si amorphous novel adsorbents. J. Mater. Res. Technol. 8, 5301–5313.

Abdelrahman, E.A., Hegazey, R.M., 2019. Utilization of waste aluminum cans in the fabrication of hydroxysodalite nanoparticles and their chitosan biopolymer composites for the removal of Ni(II) and Pb(II) ions from aqueous solutions: Kinetic, equilibrium, and reusability studies. Microchem. J. 145, 18–25.

Abdelrahman, E.A., Hegazey, R.M., 2019. Exploitation of Egyptian insecticide cans in the fabrication of Si/Fe nanostructures and their chitosan polymer composites for the removal of Ni(II), Cu(II), and Zn(II) ions from aqueous solutions. Compos. Part B Eng. 166, 382–400.

Abdelrahman, E.A., Hegazey, R.M., Alharbi, A., 2020. Facile Synthesis of Mordenite Nanoparticles for Efficient Removal of Pb(II) Ions from Aqueous Media. J. Inorg. Organomet. Polym. Mater. 30, 1369–1383.

Abdelrahman, E.A., Alharbi, A., Subaihi, A., Hameed, A.M., Almutairi, M.A., Algethami, F.K., Youssef, H.M., 2020. Facile fabrication of novel analcime/sodium aluminum silicate hydrate and zeolite Y/faujasite mesoporous nanocomposites for efficient removal of Cu(II) and Pb(II) ions from aqueous media. J. Mater. Res. Technol. 9, 7900–7914.

Abdelrahman, E.A., Subaihi, A., 2020. Application of Geopolymers Modified with Chitosan as Novel Composites for Efficient Removal of Hg(II), Cd(II), and Pb(II) Ions from Aqueous Media. J. Inorg. Organomet. Polym. Mater. 30, 2440–2463.

Abdelrahman, E.A., Abou El-Reash, Y.G., Youssef, H.M., Kotp, Y. H., Hegazey, R.M., 2021. Utilization of rice husk and waste aluminum cans for the synthesis of some nanosized zeolite, zeolite/zeolite, and geopolymer/zeolite products for the efficient removal of Co(II), Cu(II), and Zn(II) ions from aqueous media. J. Hazard. Mater. 401, 123813.

Adamovich, S.N., Filatova, E.G., Pozhidaev, Y.N., Ushakov, I.A., Chugunov, A.D., Oborina, E.N., Rozentsveig, I.B., Verpoort, F., 2021. Natural zeolite modified with 4-(3-triethoxysilylpropyl) thiosemicarbazide as an effective adsorbent for Cu(II), Co(II) and Ni(II). J. Taiwan Inst. Chem. Eng. 129, 396–409.

Ainscough, T.J., Alagappan, P., Oatley-Radcliffe, D.L., Barron, A.R., 2017. A hybrid super hydrophilic ceramic membrane and carbon nanotube adsorption process for clean water production and heavy metal removal and recovery in remote locations. J. Water Process Eng. 19, 220–230.

Altowayti, W.A.H., Othman, N., Goh, P.S., Alshalif, A.F., Al-Gheethi, A.A., Algaifi, H.A., 2021. Application of a novel nanocomposites carbon nanotubes functionalized with mesoporous silica-nitrenium ions (CNT-MS-N) in nitrate removal: Optimizations and nonlinear and linear regression analysis. Environ. Technol. Innov. 22, 101428.

Amini-Fazl, M.S., Barzegarzadeh, M., Mohammadi, R., 2021. Surface Modification of Graphene Oxide with Crosslinked Polymethacrylamide via RAFT Polymerization Strategy: Effective Removal of Heavy Metals from Aqueous Solutions. J. Inorg. Organomet. Polym. Mater. 31, 2959–2970.

Ashokkumar, M., Cavalieri, F., Chemat, F., Okitsu, K., Sambandam, A., Yasui, K., Zisu, B., 2016. Handbook of ultrasonics and sonochemistry. Handb. Ultrason. Sonochemistry. Springer 814–838.

Bashir, A., Malik, L.A., Ahad, S., Manzoor, T., Bhat, M.A., Dar, G. N., Pandith, A.H., 2019. Removal of heavy metal ions from aqueous system by ion-exchange and biosorption methods. Environ. Chem. Lett. 17, 729–754.

Cerrahoğlu, E., Kayan, A., Bingöl, D., 2017. New Inorganic-Organic Hybrid Materials and Their Oxides for Removal of Heavy Metal Ions: Response Surface Methodology Approach. J. Inorg. Organomet. Polym. Mater. 27, 427–435.

Chang, X., Jiang, N., Zheng, H., He, Q., Hu, Z., Zhai, Y., Cui, Y., 2007. Solid-phase extraction of iron(III) with an ion-imprinted functionalized silica gel sorbent prepared by a surface imprinting technique. Talanta 71, 38–43.

Chen, C., Liu, H., Chen, T., Chen, D., Frost, R.L., 2015. An insight into the removal of Pb(II), Cu(II), Co(II), Cd(II), Zn(II), Ag(I), Hg (I), Cr(VI) by Na(I)-montmorillonite and Ca(II)-montmorillonite. Appl. Clay Sci. 118, 239–247.

Correcher, V., Garcia-Guinea, J., Bustillo, M.A., Garcia, R., 2009. Study of the thermoluminescence emission of a natural α-cristobalite. Radiat. Eff. Defects Solids. 164, 59–67.

Denizli, A., Garipcan, B., Karabakan, A., Say, R., Emir, S., Patir, S., 2003. Metal-complexing ligand methacryloylamidocysteine containing polymer beads for Cd(II) removal. Sep. Purif. Technol. 30, 3–10.

Efome, J.E., Rana, D., Matsuura, T., Lan, C.Q., 2019. Effects of operating parameters and coexisting ions on the efficiency of heavy metal ions removal by nano-fibrous metal-organic framework membrane filtration process. Sci. Total Environ. 674, 355–362.

Elgueta, E., Sánchez, J., Dax, D., Xu, C., Willför, S., Rivas, B.L., González, M., 2016. Functionalized galactoglucomannan-based hydrogels for the removal of metal cations from aqueous solutions. J. Appl. Polym. Sci. 133, 1–8.

Febrianto, J., Kosasih, A.N., Sunarso, J., Ju, Y.H., Indraswati, N., Ismadji, S., 2009. Equilibrium and kinetic studies in adsorption of heavy metals using biosorbent: A summary of recent studies. J. Hazard. Mater. 162, 616–645.

Hameed, A.M., Alharbi, A., Abdelrahman, E.A., Mabrouk, E.M., Hegazey, R.M., Algethami, F.K., Al-Ghamdi, Y.O., Youssef, H. M., 2020. Facile Hydrothermal Fabrication of Analcime and Zeolite X for Efficient Removal of Cd(II) Ions From Aqueous Media and Polluted Water. J. Inorg. Organomet. Polym. Mater. 30, 4117–4128.

Kenawy, I.M., Hafez, M.A.H., Ismail, M.A., Hashem, M.A., 2018. Adsorption of Cu(II), Cd(II), Hg(II), Pb(II) and Zn(II) from aqueous single metal solutions by guanyl-modified cellulose. Int. J. Biol. Macromol. 107, 1538–1549.

Khalifa, M.E., Abdelrahman, E.A., Hassanien, M.M., Ibrahim, W.A., 2020. Application of Mesoporous Silica Nanoparticles Modified with Dibenzoylmethane as a Novel Composite for Efficient Removal of Cd(II), Hg(II), and Cu(II) Ions from Aqueous Media. J. Inorg. Organomet. Polym. Mater. 30, 2182–2196.

Liang Liao, Z., Chao Zhao, Z., Cheng Zhu, J., Chen, H., Zong Meng, D., 2021. Complexing characteristics between Cu(Ⅱ) ions and dissolved organic matter in combined sewer overflows: Implications for the removal of heavy metals by enhanced coagulation. Chemosphere. 265.

Liu, D., Yuan, Y., Wei, Y., Zhang, H., Si, Y., Zhang, F., 2022. Removal of refractory organics and heavy metals in landfill leachate concentrate by peroxi-coagulation process. J. Environ. Sci. (China) 116, 43–51.

Ma, J., Wang, H., Li, D., Liu, L., Yang, H., 2021. Preparation novel mercaptotriazole-functionalized paramagnetic nickel-zinc ferrite microspheres for absorbing Hg (II) in waste water. Colloids Surfaces A Physicochem. Eng. Asp. 616, 126324.

Malik, L.A., Bashir, A., Qureashi, A., Pandith, A.H., 2019. Detection and removal of heavy metal ions: a review. Environ. Chem. Lett. 17, 1495–1521.

Malik, D.S., Jain, C.K., Yadav, A.K., 2017. Removal of heavy metals from emerging cellulosic low-cost adsorbents: a review. Appl. Water Sci. 7, 2113–2136.

Moja, N.T., Mishra, S.B., Hwang, S.S., Tsai, T.Y., Mishra, A.K., 2021. Coordination of Lead (II) and Cadmium (II) Ions to Nylon 6/Flax Linum Composite as a Route of Removal of Heavy Metals. J. Inorg. Organomet. Polym. Mater. 31, 4532–4545.

Monier, M., Abdel-Latif, D.A., 2012. Preparation of cross-linked magnetic chitosan-phenylthiourea resin for adsorption of Hg(II), Cd(II) and Zn(II) ions from aqueous solutions. J. Hazard. Mater. 209–210, 240–249.

Mudhoo, A., Garg, V.K., Wang, S., 2012. Removal of heavy metals by biosorption. Environ. Chem. Lett. 10, 109–117.

Najafi, F., 2015. Removal of zinc(II) ion by graphene oxide (GO) and functionalized graphene oxide–glycine (GO–G) as adsorbents from aqueous solution: kinetics studies. Int. Nano Lett. 5, 171–178.

Osińska, M., 2017. Removal of lead(II), copper(II), cobalt(II) and nickel(II) ions from aqueous solutions using carbon gels. J. Sol-Gel Sci. Technol. 81, 678–692.

Saad, D.M., Cukrowska, E.M., Tutu, H., 2013. Selective removal of mercury from aqueous solutions using thiolated cross-linked polyethylenimine. Appl. Water Sci. 3, 527–534.

Shah, R.K., Naglah, A.M., Al-Omar, M.A., Almehizia, A.A., AlReshaidan, S., Subaihi, A., Alharbi, A., Hameed, A.M., Alkabli, J., Fetoh, M.E., Alluhaybi, A.A., Al-Wasidi, A.S., Alraddadi, T.S., Youssef, H.M., 2021. Efficient removal of Ni(II) ions from aqueous solutions using analcime modified with dimethylglyoxime composite. Arab. J. Chem. 14, 103197.

Shamim, M.A., Zia, H., Zeeshan, M., Khan, M.Y., Shahid, M., 2022. Metal organic frameworks (MOFs) as a cutting-edge tool for the selective detection and rapid removal of heavy metal ions from water: Recent progress. J. Environ. Chem. Eng. 10, 106991.

Sharma, A., Anjana, H., Rana, S.G., 2022. A Comprehensive Review on the Heavy Metal Removal for Water Remediation by the Application of Lignocellulosic Biomass-Derived Nanocellulose. J. Polym. Environ. 30, 1–18.

Shawabkeh, R., 2009. Equilibrium study and kinetics of Cu^{2+} removal from water by zeolite prepared from oil shale ash. Process Saf. Environ. Prot. 87, 261–266.

Sheng, P.X., Ting, Y.P., Chen, J.P., Hong, L., 2004. Sorption of lead, copper, cadmium, zinc, and nickel by marine algal biomass: Characterization of biosorptive capacity and investigation of mechanisms. J. Colloid Interface Sci. 275, 131–141.

Sobhanardakani, S., Zandipak, R., Cheraghi, M., 2015. Adsorption of Cu^{2+} Ions From Aqueous Solutions Using Oxidized Multi-Walled Carbon Nanotubes. Avicenna J. Environ. Heal. Eng. 2, 1–6.

Sobhanardakani, S., Zandipak, R., 2015. 2,4-Dinitrophenylhydrazine functionalized sodium dodecyl sulfate-coated magnetite nanoparticles for effective removal of Cd(II) and Ni(II) ions from water samples. Environ Monit Assess. 187, 412.

Sobhanardakani, S., Zandipak, R., Javad, M., 2016. Removal of Ni (II) and Zn(II) from Aqueous Solutions Using Chitosan. Arch. Hygiene Sci. 5, 47–55.

Sobhanardakani, S., Ahmadi, M., Zandipak, R., 2016. Efficient removal of Cu(II) and Pb(II) heavy metal ions from water samples using 2,4-dinitrophenylhydrazine loaded sodium dodecyl sulfate-coated magnetite nanoparticles. J. Water Supply Res. Technol. - AQUA. 65, 361–372.

Sobhanardakani, S., Jafari, A., Zandipak, R., Meidanchi, A., 2018. Removal of heavy metal (Hg(II) and Cr(VI)) ions from aqueous solutions using Fe_2O_3@SiO_2 thin films as a novel adsorbent. Process Saf. Environ. Prot. 120, 348–357.

Sobhanardakani, S., Zandipak, R., 2017. Synthesis and application of $TiO_2/SiO_2/Fe_3O_4$ nanoparticles as novel adsorbent for removal of Cd(II), Hg(II) and Ni(II) ions from water samples. Clean Technol. Environ. Policy. 19, 1913–1925.

Talebzadeh, F., Zandipak, R., Sobhanardakani, S., 2016. CeO2 nanoparticles supported on CuFe2O4 nanofibers as novel adsorbent for removal of Pb(II), Ni(II), and V(V) ions from petrochemical wastewater. Desalin. Water Treat. 57, 28363–28377.

Tan, G., Xiao, D., 2009. Adsorption of cadmium ion from aqueous solution by ground wheat stems. J. Hazard. Mater. 164, 1359–1363.

Valle, H., Sánchez, J., Rivas, B.L., 2015. Poly(N-vinylpyrrolidone-co-2-acrylamido-2-methylpropanesulfonate sodium): Synthesis, characterization, and its potential application for the removal of metal ions from aqueous solution. J. Appl. Polym. Sci. 132, 1–7.

Xu, Z.P., Braterman, P.S., 2003. High affinity of dodecylbenzene sulfonate for layered double hydroxide and resulting morphological changes. J. Mater. Chem. 13, 268–273.

Xue, S.-H., Xie, H., Ping, H., Li, Q.-C., Su, B.-L., Fu, Z.-Y., 2015. Induced Transformation of Amorphous Silica to Cristobalite on Bacterial Surface. Rsc Adv. 5, 71844–71848.

Youssef, H.M., Shah, R.K., Algethami, F.K., Hegazey, R.M., Naglah, A.M., Al-Omar, M.A., Alluhaybi, A.A., Alherbish, H.A., Mabrouk, E.M., Abdelrahman, E.A., 2021. Facile Hydrothermal Procedure for the Synthesis of Sodium Aluminum Silicate Hydrate/Analcime and Analcime for Effective Removal of Manganese(II) Ions From Aqueous Solutions. J. Inorg. Organomet. Polym. Mater. 31, 1035–1046.